DNA Cholesteric Phases: The Role of DNA Molecular Chirality and DNA−DNA Electrostatic Interactions

A. G. Cherstvy*

Institut für Festköperforschung, Theorie-II, Forschungszentrum Jülich, D-52425 Jülich, Germany, and Max-Planck-Institut für Physik komplexer Systeme, Nöthnitzer Straβe 38, D-01187 Dresden, Germany

Received: February 11, 2008; Revised Manuscript Received: May 21, 2008

DNA molecules form dense liquid-crystalline twisted phases both in vivo and in vitro. How the microscopic DNA chirality is transferred into intermolecular twist in these mesophases and what is the role of chiral DNA−DNA electrostatic interactions is still not completely clear. In this paper, we first give an extended overview of experimental observations on DNA cholesteric phases and discuss the factors affecting their stability. Then, we consider the effects of steric and electrostatic interactions of grooved helical molecules on the sign of cholesteric twist. We present some theoretical results on the strength of DNA−DNA chiral electrostatic interactions, on DNA−DNA azimuthal correlations in cholesteric phases, on the value of DNA cholesteric pitch, and on the regions of existence of DNA chiral phases stabilized by electrostatic interactions. We suggest for instance that 146 bp long DNA fragments with stronger affinities for the nucleosome formation can form less chiral cholesteric phases, with a larger left-handed cholesteric pitch. Also, the value of left-handed pitch formed in assemblies of homologous DNA fragments is predicted to be smaller than that of randomly sequenced DNAs. We expect also the cholesteric assemblies of several-kbp-long DNAs to require higher external osmotic pressures for their stability than twisted phases of short nucleosomal DNA fragments at the same DNA lattice density.

1. Introduction

Many rod-like biomacromolecules are chiral in nature and some of them are capable of forming dense cholesteric phases (CPs). Among them are the fragments of DNA,[1−5] some filamentous proteins (chitin and collagen), cellulose and some its derivatives, some cylindrical viruses (fd and M13),[6] flagella filaments,[7] some synthetic polypeptides (poly-γ-benzyl-L-glutamate PBLG),[8,9] and polysaccharides (xanthan and schizophyllan).[10] Not all chiral molecules form CPs, and often the nematic phases only are observed for these elongated particles, like for tobacco mosaic virus TMV.[11] Many of these helices have a grooved structure as well as quite high electric charges. How the molecular chirality manifests itself in macroscopic properties of the chiral phases formed and which intermolecular interactions are responsible for that is still not fully understood.[12,13]

Concentrated solutions of DNA molecules under proper conditions form CPs,[14,15] Figure 1. In vivo, DNA in chromosomes of some bacteria and dinoflagellates (unicellular algae) reveals a cholesteric organization.[3,16] In vitro, the properties of DNA CPs have been extensively studied in several laboratories over the last couple of decades. Smectic phases that are observed in solutions of some monodisperse viruses (TMV) are not common for polydisperse DNA solutions used in experiments.

This paper is organized as follows. First, we discuss the directions of the cholesteric twist caused by steric and electrostatic interactions (EIs) acting between some model grooved charged helices. Then, we present an extended overview of experimental observations regarding the properties of DNA CPs. We concentrate on the effects of binding of mono- and multivalent cations on DNA as well as of charged flexible DNA-binding polymers on the sign and magnitude of DNA cholesteric pitch. Then, we overview the recent progress in understanding of effects of EIs in dense phases of DNAs and of some helical viruses. Afterward, we give an introduction into the theory of DNA−DNA chiral EIs and present some of its consequences. We contrast theoretical results with experimental observations for DNA CPs. We modify this linear electrostatic theory to include some additional salt effects inherent for dense DNA assemblies. Within the ground-state energy model for a triad of DNAs, we present the results for DNA cholesteric pitch and for the regions of stability of DNA twisted phases stabilized by EIs. We calculate the densities of DNA assemblies with strong azimuthal DNA−DNA correlations. We put forward some predictions about the value of DNA cholesteric pitch for assemblies of homologous vs randomly sequenced DNA fragments. In the last section, we discuss some universal aspects of chiral EIs on formation of CPs.

1.1. Steric Interactions of Helices. In closely packed lattices of nearly parallel helices, steric interactions between them can stabilize the CP formation. The well-known proposition of Straley is that right-handed grooved helices preferably form left-handed CPs.[17] Doing so, twisted helices in close contact can avoid crossings of their ridges. That can stabilize CPs over the nematic ones.[18] This conjecture is often used to explain the experimental fact that right-handed B-DNAs form exclusively left-handed CPs. This conclusion is correct for helices that cross at a proper angle and have proper relations between the helix diameter, pitch, and groove depth. It is however incorrect in general, particularly for helices with a large diameter.

Grooved right-handed helices with a small helix inclination angle $\alpha < \pi/4$ and large radius should form preferentially right-handed CPs, Figure 2a. That provides less steric clashes of ridges/protrusions on the contacting molecular surfaces. For right-handed helices with $\alpha > \pi/4$, the left-handed phases should

* To whom correspondence should be addressed. E-mail: a.cherstvy@fz-juelich.de.

10.1021/jp801220p CCC: $40.75
Published on Web 09/12/2008

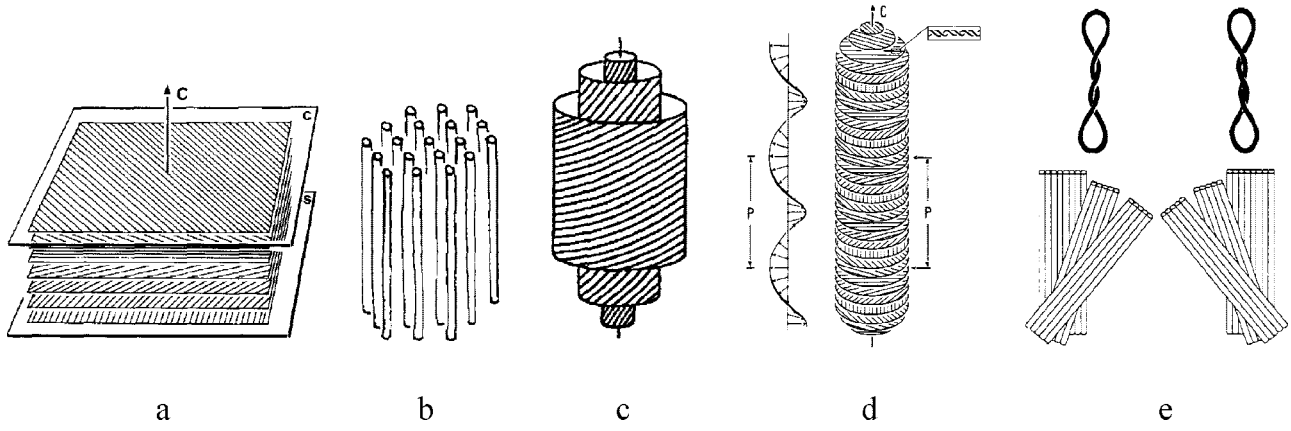

Figure 1. Schematic structure of DNA dense phases observed in vivo and in vitro. (a) Left-handed simple-twist DNA CP. (b) DNA columnar hexagonal phase. (c) Double twisted DNA blue CP (reprinted from ref 1). (d) Structure of dinoflagellate chromosome (reprinted from ref 3 with permission from American Chemical Society). (e) DNA CPs formed by supercoiled DNAs (reprinted from ref 37 with permission from Wiley-Liss, Inc., a subsidiary of John Wiley Sons, Inc.).

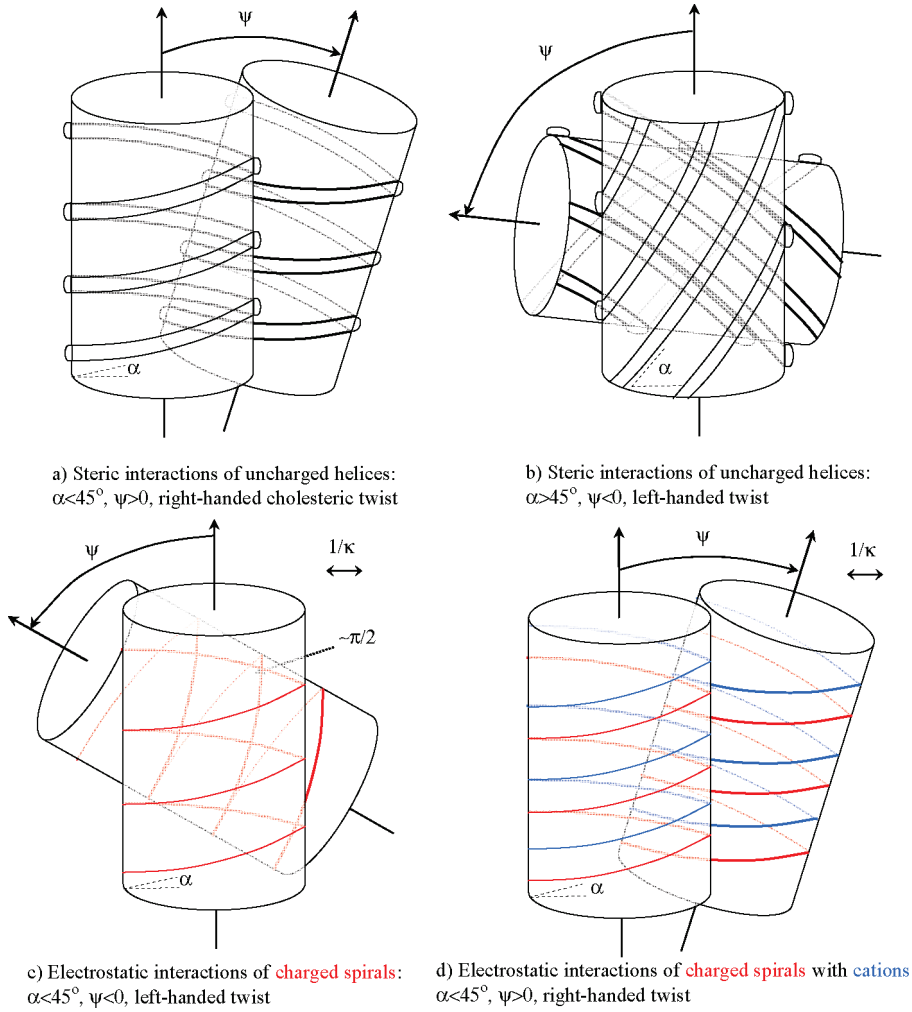

Figure 2. Scheme showing how steric (top pictures) and EIs (bottom pictures) can affect the handedness of CPs of densely packed right-handed helices with large diameters. The ridges on the contacting sides of helices are drawn as thicker curves. The helix inclination angle is α, the mutual twist angle of helices is Ψ.

be preferred, Figure 2b. Similar packing requirements govern the fitting of α helices into each other upon formation of dense protein structures. Namely, a mutual twist rotation of closely packed α helices is required to provide a proper fitting of ridges formed by amino acids on one helix into the grooves on the neighboring helix.[19] So, depending on the value of the helix opening angle α, right-handed helices can form either right- or left-handed twist phases.[20]

These steric fitting rules work for ideal thick densely packed helices. In reality, however, nucleosomal ~150 bp long DNA fragments[15,21] as well as M13 viruses[22] are right-handed helices with $\alpha < 45°$, but they are known to form predominantly left-handed CPs. As for DNA CPs, the DNA−DNA surface-to-surface separations are 15−25 Å, the steric hindrance of contacting DNA grooves is unlikely to be the dominant factor for stability of these phases. Forces of a longer range should contribute.

1.2. Electrostatic Interactions. Many helices forming CPs have well recognized helical charge patterns, with a high overall surface charge density. The chiral EIs of these patterns can serve as the long-range forces stabilizing the CPs. Indeed, for dense DNA columnar hexagonal lattices, the measured pressure−distance curves[23] reveal quantitative agreement with the results of theory of EIs between parallel charged DNA duplexes.[24] For two skewed charged spirals, the chiral EIs can favor orientations opposite to that of steric repulsion. Namely, two charged lines minimize their EIs at perpendicular orientation.[25] Now, imagine two negatively charged right-handed helices with $\alpha < \pi/4$ and large diameter interacting in high-salt electrolytes. Then, only two neighboring spiral fragments contribute substantially to the helix-helix EI energy. Perpendicular local orientation of these fragments will be favored, Figure 2c, and thus a left-handed CP is expected. In low-salt limit, more charges further away from spiral−spiral contact interact efficiently and thus a tendency to have perpendicular orientation of helical axes emerges. The combination of the two effects gives the final value of the twist angle.

Of course, the charge pattern on DNA is more complex than that of a uniformly charged spiral or of an ideal helical array of point-like charges.[26] It contains also positive charges of counterions which are adsorbed onto highly negatively charged DNA from solution. This affects simple electrostatic conclusions listed above, both for sign and salt dependence of the cholesteric pitch. Namely, many cations adsorbing onto the DNA form charged strings in DNA grooves and compensate for a major fraction of DNA charge. Therefore, for two skewed spirals, strings of negative phosphate charges on one spiral prefer to be aligned locally more parallel to the strings of cations in the grooves of another spiral. Thus, two right-handed nearly net-neutral spirals, formed by DNA phosphate strings and by cations adsorbed in the grooves, with $\alpha < \pi/4$ will likely prefer to form right-handed CPs over the left-handed ones, Figure 2d. The right-handed twist direction indeed follows from the accurate theory of DNA−DNA chiral EIs considered below.

B-DNA also is not fully neutralized by adsorbed cations and it has a double-helical structure with two unequal grooves. The force balance between electrostatic torque that favors a finite twist angle Ψ between DNAs and the tendency to form columnar hexagonal phases, governs the final twist angle between DNAs. The second tendency is due to a longer effective interaction length for EIs between parallel DNAs as compared to the skewed ones, that affects the cholesteric pitch especially for conditions of DNA−DNA attraction. We address the reader to the most involved theory of chiral EIs of helical molecules developed so far, refs 13 and 27. Below, we use and modify this theory to describe some properties of DNA CPs.

It is well-known that CPs of chiral molecules are characterized by short-range positional and long-range orientational correlations. The latter are vital for existence of CPs[20] because otherwise the chiral component of intermolecular interactions would be washed out being averaged over all possible azimuthal orientations of molecules in the assembly. Although for DNA CPs the strength of azimuthal correlations has not been directly measured, they are expected to decrease at higher salinities.[28]

2. DNA Cholesteric Phases: Experimental Observations and Some Predictions

2.1. Linear DNA with Mono- and Multivalent Cations. Extensive studies of dense CPs of B-DNA, with DNA concentrations [DNA] between 160 and 290−350 mg/mL, under the stabilizing osmotic stress of poly(ethylene glycol) (PEG) solution have been performed.[21] At larger [DNA], columnar hexagonal phases were observed, whereas at smaller DNA densities, the blue and isotropic phases were detected. For ~500 Å long DNA fragments at [DNA] from 160 to 220 mg/mL, the isotropic and CPs are known to coexist.[29] The DNA concentrations C_i (when the anisotropic phase first appears) and C_a (when the last isotropic fraction disappear) were shown to depend only weakly on electrolyte concentration n_0, slightly increasing when n_0 increases from 0.01 to 1 M.[29] Longer DNAs reveal a stronger dependence of $C_{i,a}$ on n_0.

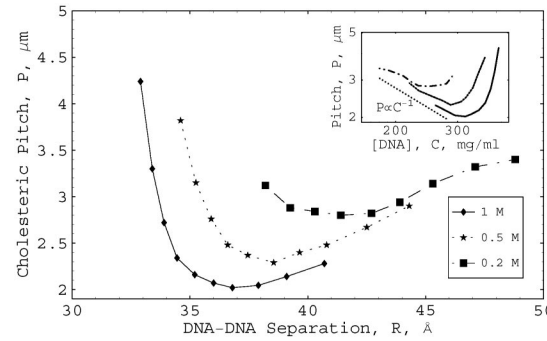

Figure 3. Experimental data on DNA cholesteric pitch variation with the density of dense assemblies of 146-bp-long DNA fragments at different salt concentrations (0.2, 0.5, and 1 M). The data are taken from Figure 5a of ref 32, with permission of the Biophysical Society. The scaling prediction for concentration dependence of the pitch at low [DNA] for the same data, $P \propto 1/C$, is presented as a dotted line in the insert.

The cholesteric pitch of solutions of short ~150 bp nucleosomal DNA fragments is reported to be left-handed, with the value of $P \sim 2-4$ μm.[30−32] In CPs the DNAs form locally a hexagonal lattice with the twist angle between DNAs of 0.3−0.7°. High-molecular weight solutions of PEG, that are excluded from the DNA phase, are typically used to exert stresses on DNA assemblies. Smaller pitch $P \sim 0.2-0.4$ μm is observed in the presence of K^+ or NH_4^+.[15] The pitch is nearly independent of DNA length for $L \sim 150-9000$ bp in polydisperse DNA solutions as well as on the initial [DNA] in solution.

The detailed measurements of $P(n_0)$ were performed on DNA cholesteric spherulites made from monodisperse ~150 bp DNA fragments.[32] The CPs were shown to be stable for DNA−DNA separations 38 Å $\lesssim R \lesssim$ 50 Å at $n_0 = 0.2$ M and at 32 Å $\lesssim R \lesssim$ 40 Å at 1 M of salt, Figure 3. This shift of stability region is consistent with the general effect of DNA−DNA EIs: at higher [salt] charge screening effects are stronger that shifts the region of strong DNA−DNA azimuthal correlations to smaller R. The pitch however decreases with increase of n_0 from 0.2 to 1 M, counter-intuitively to a naive expectation of weaker chiral interactions at higher [salt]. The explanation suggested originally is that at lower n_0 the helical charge pattern on DNA is smeared out, which results in weaker chiral DNA−DNA EIs.[32] Note here that the $P(n_0)$ dependence observed for DNA is not universal for other helices. Namely, for CPs of PEG-coated fd-viruses at low [virus] the P values increase at higher [salt].[12]

DNA cholesteric pitch behaves nonmonotonously with the density of DNA lattice. It increases considerably at the boundaries of cholesteric−isotropic and cholesteric−hexagonal phase transitions.[32,29] No explanation has been suggested so far for this reduction of DNA clear pitch at higher salt amounts and for a shift of DNA CPs toward lower [DNA] at higher n_0.

In the presence of di- and trivalent cations, the pitch values reported up to 10 times larger than in NaCl solutions, up to P

$\sim 22\ \mu$m.[21] Some of multivalent cations studied do not condense DNA (Mg^{2+} and Ca^{2+}), while the others do induce DNA condensation (spermine^{4+} and spermidine^{3+}). One can argue whether different patterns of counterion binding onto DNA, Na vs spermidine, can trigger this dramatic pitch increase in the presence of multivalent cations. Note that the pitch in solutions with spermidine^{3+} decreases dramatically with temperature, from $\sim 22\ \mu$m at 20° down to $\sim 4\ \mu$m at 65°.[33]

2.2. DNA with Oppositely Charged Polymers. Short DNA fragments form predominantly left-handed CPs, both in solutions of mono- and multivalent cations. More complex behavior is detected for DNA CPs with positively charged short polymers. For instance, DNA complexes with helical polymer chitosan reveal a reversal in pitch sign, from a left- to a right-handed one.[35] It was suggested that, depending on distribution of charges on chitosan as well as on the type of its interactions with DNA, some dipolar structures are formed along DNA in DNA−chitosan complexes. Interactions of these dipoles might then cause a change in the twist sense. Similar dipole−dipole interactions might be responsible for a pitch reversal in DNA complexes with cationic intercalator daunomycin.[36] In particular, at [daunomycin] $< 8\ \mu$M the CPs are left-handed, whereas they become right-handed at larger concentrations.[4]

The pitch reversal occurs also for DNAs with positively charged poly(lysine),[37] depending on the handedness of peptides and on the amount of added salt. These peptides, acting like linear cations on the DNA, can bind along the duplex (in a helical manner) and also bridge two DNAs together.[38] The influence of other DNA groove-binders and intercalators on the pitch value was also studied.[39−41] To what extent the charge distribution of polycations and drugs bound on DNA affects the properties of CPs formed is however still not clear. For instance, why do extended linear polyamines fail to induce the pitch inversion, while other positively charged polymers are capable of doing this? Or why some uncharged daunomycin homologues are capable to trigger the pitch inversion as well?

2.3. Supercoiled and Curved DNA: Predictions for Cholesteric Pitch of Bent Nucleosomal DNA Fragments. The DNAs of several kbp in length, both linear and bacterial plasmids, form CPs as well.[37] The formation of CPs by supercoiled DNA in vivo is an effective mechanism of DNA packaging in some bacteria[42] and viruses.[44] The X-ray scattering study on intact *E. coli* has revealed that positive supercoiling of bacterial plasmids induces long-range left-handed cholesteric DNA organization.[42] CPs of supercoiled DNAs are stable at lower [DNA] as compared to those of linear DNAs. The assemblies of supercoiled DNAs in vitro reveal a change of P sign from right- to left-handed as [salt] grows.[37] Right-handed DNA supercoils were shown to form predominantly left-handed phases, and vice versa, Figure 1e. That is in agreement with the steric fitting rule of two helices with large inclination angles representing each strand of supercoiled DNA, Figure 2b.[43] The pitch of CPs of supercoiled DNAs is more sensitive to solution parameters than that of linear DNAs.[44] The pitch reversal can be triggered by intercalating agents that unwind DNA upon binding.

Not only fine molecular details affect the P value, the 3D shape of helices in space can have an effect as well. For instance, for fd-phage coated with PEG a superhelical path of the molecule was suggested to contribute to the observed P value and sign.[12] One can speculate that intrinsic curvature of 146 bp nucleosomal DNA fragments, often used to study DNA CPs in vitro, can affect the cholesteric pitch value in a similar fashion. Namely, being wrapped in nucleosomes, DNA takes a left-handed superhelical path. DNA binding to histones is at least partly governed by sequence specific DNA elastic deformations, both of static and of dynamical nature.

Static, intrinsic bends in DNA structure are known to facilitate DNA binding to histones.[45] Negatively supercoiled DNA as well as DNA fragments prebent in the same direction bind to histones stronger than straight DNA fragments,[46,47] due to a lower mechanical bending energy of DNA wrapping. Particular bp-combinations are known to induce considerable bends in the duplex, for instance, short stretches of dA or dT bps. Also, it is known that DNA sequences with strong affinity to nucleosomes reveal quite periodic distribution of A/T and C/G bps, with the period of about 10 bps. The A/T bps occur more often when the DNA minor groove faces toward the histone octamer, while C/G bps are more abundant when the DNA minor groove points outward the core.[48,49]

Dynamical bp-specific DNA bendability, anisotropic flexibility, is another mechanism that contributes to DNA affinity to nucleosomes.[50,51] Here, periodic A/T and C/G modulations on nucleosomal DNA fragments are validated by the fact that A/T bps are easily compressible into the minor groove, whereas C/G bps reveal easier major groove compression.[52] The relative contribution of these two factors for positioning of nucleosomes on DNA is still not completely clear, although DNA bendability seems to be more important.

To our knowledge, no detailed measurements of conformations of 146 bp-long DNA sequences in solutions have been performed for DNA fragments with different affinities to nucleosomes. Static curvature effects for DNA fragments were measured for a number of repetitive sequences running through the gels via electrophoresis.[53] It was shown that particular 10 bp-long-repeats with A/T bp stretches have revealed anomalously slow migration through the gel. This was attributed to a superhelical path taken by such DNA fragments in space, that is induced by a periodic occurrence of bps inducing DNA bends. The radius of these DNA superhelices r was consistent with the velocity of DNA permeation through the gel, up to $r \sim 50-70$ Å for the slowest DNA fragments.

Although DNA sequences bound to nucleosomes are not perfectly repetitive, they do contain a $\sim$10 bp periodic motive in positioning of A/T and G/C bps. This can result in formation of DNA superhelices or other regularly curved structures for DNA fragments released form the histone core. Theoretical calculations of the actual shapes for DNA sequences strongly bound to nucleosomes (nucleosome positioning sequences) and the analysis of effects of this curvature onto affinity of DNA fragments to the histones is a separate problem. It requires the knowledge of equilibrium DNA bp geometrical parameters as well as DNA bp-dependent flexibility constants. Both of them can be extracted from X-ray data on crystals of DNA oligomers and of DNA complexes with proteins,[54,55] see also ref 56.

One possibility is that the DNA anisotropic flexibility dominates bp specific effects in DNA bending around nucleosomes. Then, after unbinding from the core, the superhelical path of DNA is expected to relax to a nearly straight rod on a microsecond time scale.[57] More likely however is that the unwrapped DNAs still keep some residual left-handed superhelicity, with the angles $\alpha > \pi/4$, preserving the shape of DNA on the length-scales $\gg H$. Therefore, as dense solutions of such fragments are compressed by external osmotic stresses, this superhelicity should shift the sense of DNA CPs toward being more right-handed.

The hypothesis is that, at the same density of DNA lattice, the DNA fragments with a strong affinity to histones (strongly

curved superhelices) should form left-handed CPs with larger, more positive pitch values than those with a lower histone affinity (weakly curved DNAs). This steric contribution from DNA superhelical shape thus counteracts the tendency of formation of left-handed CPs coming from long-range DNA−DNA interactions. It would be interesting to test experimentally whether the cholesteric pitch for strongly and weakly bound nucleosomal DNA fragments indeed differs substantially. Note here that a pronounced DNA superhelicity is expected also to decrease the density of DNA assembly and thereby also to affect the equilibrium value of the cholesteric pitch.

2.4. DNA Chiral Organization in Viruses and Sperm. DNA packaging inside many bacteriophages involves a close juxtaposition of DNAs, with $R \sim 24-28$ Å.[58−61] DNA confinement imposed by viral shells ensures tremendous DNA packing densities inside such viruses. On the other hand, small volumes available inside the shells distort locally hexagonal DNA packing. Several models of DNA organization inside viruses have been suggested in the literature, with the DNA spool model being the broadly accepted one. Dense cholesteric DNA domains can also occur inside viruses,[60] with indication of left-handed DNA CPs for some phages. It is however not clear how strongly the chiral DNA−DNA interactions affect the properties of DNA packaging inside viruses.

DNA is packed chirally also inside sperm of some higher eukaryotes (horse, human).[62] Here, DNA is compactified by positively charged protamines to a very high density, with $R \approx 25-28$ Å. These distances are close to those observed in DNA toroids with multivalent cations[63] and predicted by the theory of EIs of parallel DNA duplexes.[64,24,65] DNA packaged in sperm reveals both columnar hexagonal phase and double-twisted CP.[62] In the latter, Figure 1c, DNAs form an elongated condensate, with DNA layers wrapped around a common axis. The pitch of these *in vivo* left-handed structures is only ∼66 nm, that gives local twist angle of neighboring DNA layers up to 16°. These large angles destroy hexagonal order in DNA lattice already after several DNA layers wrapped.

3. DNA Cholesteric Phases: Electrostatic Interactions and Theoretical Results

3.1. Recent Numerical Results. For CPs formed by M13 viruses, the numerical procedure of summation of EIs acting between viral coat proteins was suggested recently in ref 22. A left-handed pitch was obtained for the right-handed viruses with helix angle $\alpha \approx 41°$, with the P values close to those observed experimentally. Also, the dependence of P on temperature and ionic strength revealed a correct tendency with some experimental data. Steric interactions, which are basically independent of n_0 and T, could not account for the experimental trends. Physical mechanisms for these pitch dependencies were however not clearly described in this paper.

For B-DNA, with $\alpha \approx 31°$, the competition of DNA−DNA steric and repulsive EIs was also recently shown to result in left-handed CPs.[66] Only negative charges on DNA have however been considered in this study, diminished in the absolute value according to the Manning's counterion condensation.[67] The effects of distribution of adsorbed cations on DNA were neglected. The absolute pitch values, its sign, and T dependence were however shown to be in qualitative agreement with some measurements. Both for M13 viruses and for B-DNAs, the EIs favoring left-handed CPs were shown to be much stronger than steric forces, favoring the opposite twist sense for these helix parameters.

3.2. Theory of Chiral EIs of DNA Duplexes. For parallel DNA duplexes, the theory of EIs has been applied for description of pressure-distance curves measured in dense columnar DNA assemblies,[24,68] decay lengths of DNA−DNA interactions, DNA condensates, and EIs between nucleosome core particles.[69] For skewed DNAs, the theory of chiral EIs has also been developed recently, both for infinitely long $L \gg H$[70,71] and for finite-length duplexes.[27,13]

In these theories, the DNAs were treated as straight rigid double spirals with a low-dielectric core and continuous helical charge patterns, both for DNA phosphates and for adsorbed cations. The latter neutralize 70−90% of DNA charge, being adsorbed either in DNA grooves or on the phosphate strands. Two such duplexes in a close juxtaposition, at 10−15 Å between the surfaces, reveal a pronounced charge alternation pattern along their surfaces that affects strongly DNA−DNA EIs.

For infinitely long fully neutralized model helices, it was suggested that the preferred mutual twist angle is right-handed, being a simple combination of helix length L, its pitch H, and helix−helix separation R[70]

$$\Psi_* \sim \sqrt{RH}/L \tag{1}$$

The theory of EIs for finite-length DNA fragments results in more complex dependence of the mutual twist angle on molecular parameters, see below.

There are three contributions in the energy of EIs of skewed DNA helices. The first is coming from the repulsion of uniformly charged cylinders with the surface charge density σ equal to that of the smeared DNA non-neutralized charge. This term favors perpendicular alignment in a pair of rods. The energy of repulsion of long skewed rods of radius a in electrolyte with Debye length $1/\kappa$ is[25,72]

$$E(\Psi) = \frac{8\pi^3\sigma^2}{\varepsilon\kappa^3 K_1^{\,2}(\kappa a)} \frac{e^{-\kappa R}}{|\sin(\Psi)|} \tag{2}$$

where Ψ is their mutual twist angle and R is the closest separation. In dense assembly, this term favors however parallel alignment of rods: in such columnar phase, the unfavorable rod-rod repulsions are reduced via maximazing intermolecular separations and avoiding close contacts that would occur for twisted configurations of cylinders.[70]

Two other contributions are due to DNA helical charge pattern. First of them originates from DNA−DNA attraction that occurs between well-neutralized DNAs at proper conditions due to structure-induced charge correlations on their surfaces. Namely, the phosphates of one DNA can be positioned in register with counterions adsorbed in the grooves of another DNA.[13] This attraction is more pronounced for DNAs with cations adsorbed in the major groove. This term favors parallel alignment of DNAs that favors maximal DNA−DNA interaction length. Second term is the chiral electrostatic torque that favors a finite value of the mutual twist angle between DNAs. The competition of all energy terms crucially depends on the value of parameters used for description of counterion pattern on DNA. It can result in nonzero DNA−DNA twist angles Ψ and thus validate the existence of DNA CPs stabilized by electrostatics.

For infinitely long DNAs,[71] the energy diverges at $\Psi \to 0$ when the interaction length becomes infinite, Figure 4. For 146 bp DNA fragments,[27] the theory of interaction of finite-length DNA helices at $L \gg H$, $R \ll L$ provides the correct energy value at $\Psi = 0$.

3.3. Approximations of the Model. We discuss here some approximations used for description of EIs of finite-length helices in DNA CPs.[27]

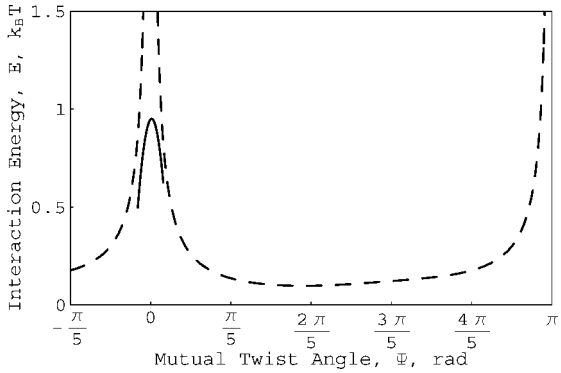

Figure 4. The energy of EIs of skewed infinitely long DNAs (dashed curve, eqs 9−11 in ref 71) and for 146 bp long DNA fragments in small angle approximation (solid curve, eqs A1−A5 in ref 27), as a function of their twist angle Ψ at the closest separation of $R = 35$ Å. The molecules are crossing in the middle and have zero azimuthal orientation angles. Parameters: the fractions of adsorbed cations in minor/major DNA grooves are 40%/60%, $1/\kappa = 7$ Å, the DNA radius is $a = 9$ Å, DNA charge compensation fraction is $\theta = 0.75$. Donnan equilibrium for DNA lattice is taken into account.

First, the pairwise nearest-neighbor summation of DNA−DNA EIs has been performed for the cholesteric pitch calculations. As DNA−DNA EIs are screened nearly exponentially and surface distances relevant for DNA CPs are typically larger than the Debye screening length, this assumption is quite reasonable.

Second, the model of molecular triad in the ground state and the approximation of small twist angles Ψ have been utilized for pitch calculations. The energy of DNA−DNA EIs in a triad can then be written as a sum of the first two terms of the expansion of EI energy of tree DNAs on a triangular lattice over angle Ψ as

$$E_{\Delta}(\Psi, R) \approx U_0(R) + U_1(R)\Psi + U_2(R)\Psi^2/2 \qquad (3)$$

This energy expansion provides the unique solution for the optimal crossing angle Ψ_*. The cholesteric pitch is obtained by minimization of this energy over Ψ [27]

$$P(R) = \frac{2\pi K_{22}}{K_t} = \frac{\sqrt{3}\pi R}{\Psi_*} = -\frac{\sqrt{3}\pi R\langle U_2\rangle}{\langle U_1\rangle} \qquad (4)$$

Here, K_{22} is the twist elastic constant of the CP and K_t is the chiral torque. The averaging $\langle\rangle$ is performed over translational and azimuthal degrees of freedom of DNAs in the assembly. Exact expressions for $U_1 = 2(u_{11} + u_{12})$ and $U_2 = 2(u_{20} + u_{21} + u_{22})$ are presented in eqs 11 and 12 of ref 27. Multiple solutions for Ψ_* are possible when further terms in the energy expansion are taken into account. This applies to situations with multiple DNA−DNA crossings in neighboring layers of the CP that are realized for long DNAs or for large Ψ values.

Third, most importantly, these ground-state pitch calculations neglect azimuthal fluctuations of DNAs on the lattice and assume perfect angular DNA−DNA correlations in DNA CPs. At finite T, DNA azimuthal fluctuations should weaken the chiral EIs and thus pitch values should increase. As these fluctuation effects depend on DNA length, in realistic statistical theory with DNA thermal motions the crucial $P(L) \propto L^2$ dependence predicted from the ground-state model can change. The fluctuations are most pronounced for short DNAs, where they can cause a much weaker final $P(L)$ dependence.[73] Such theory, that would couple the DNA azimuthal fluctuations on the lattice and DNA twist elastic deformations with chiral DNA−DNA EI potential, is a complicated statistical problem yet unsolved. For DNA columnar assemblies, the statistical mechanics has recently been developed in ref 74.

Fourth, the linear electrostatic Debye−Hueckel theory used here neglects the effects of ionic correlations in electrolyte solutions. At high [salt], that can occur inside DNA−DNA phases; however, the gas of co- and counter-ions becomes substantially nonideal due to formation of ion pairs. The concentration of free ions contributing to screening in DNA phase is therefore reduced and EIs become less screened. The subject of nonideality of electrolyte solutions in dense phases of highly charged polyelectrolytes is a separate field of research, that is beyond the scope of this paper.

Fifth, the DNAs were modeled as ideal straight spirals, without considering the effects of bp sequence on DNA charge positioning. The DNA bp parameters are however known to depend considerably on DNA bp sequence. In particular, twist angles between neighboring DNA bp steps vary between ≈28 and ≈40°, with the average of ≈36° for B-DNA with about 10 bps per turn of the helical structure.[54]

3.4. Cholesteric Pitch of Homologous and Randomly Sequenced DNA Fragments. For interaction of straight nonideal DNAs, the bp-specific variation in twist angles between neighboring bases is most important to take into account. These variations are known to affect strongly helix-specific EIs of parallel duplexes. Namely, for ideal DNAs or for homologous DNA sequences, the register of charges along the DNA contact is perfect, independently on juxtaposition length. The charge pattern on DNAs with uncorrelated sequences (e.g., for randomly sequenced DNAs) is however nonideal or corrugated. The accumulation of these structural nonidealities along the DNA distorts the charge register along the DNA−DNA contact. The DNA−DNA charge register can now be only preserved over some finite length, the helical coherence length, that is inversely proportional to the magnitude of twist angle variations of the DNA structure. To ensure DNA−DNA charge register beyond this length, some torsional adjustments of the DNA backbone are required that costs twist elastic energy. Thus, the EIs of parallel DNA fragments with noncorrelated sequences are less favorable than EIs of homologous DNA sequences.[68]

Similar effects are expected for skewed DNAs. For CPs formed by randomly sequenced DNAs one can anticipate weaker chiral DNA-DNA EIs, weaker azimuthal correlations, and larger values of the cholesteric pitch,[75] as compared to CPs formed by homologous DNA fragments (or by regular helices such as long poly(dA)·poly(dT) and poly(dG)·poly(dC) DNA tracts) at the same DNA lattice density. This prediction would be interesting to test experimentally. Note however that, along with the effects of intermolecular interactions, the pitch of DNA CPs with different bp sequences can be affected by bp-specific intrinsic DNA bends that affect the overall density of DNA CPs.

Some bp sequence effects in DNA CPs were studied recently in DNA cholesteric spherulites constructed of both homologous and nonhomologous DNA fragments.[76] It was shown in particular that homologous DNA sequences segregate into separate populations within spherulites. This is the first direct proof that interactions of DNA fragments with similar/homologous sequences are more favorable that those between nonhomologous DNA sequences. At separations of 10−20 Å between DNA surfaces, the interaction energy difference is large enough to provoke the separation of DNA molecules into different populations. The pitch values for CPs of homologous and nonhomologous DNAs have however not been compared in this study.

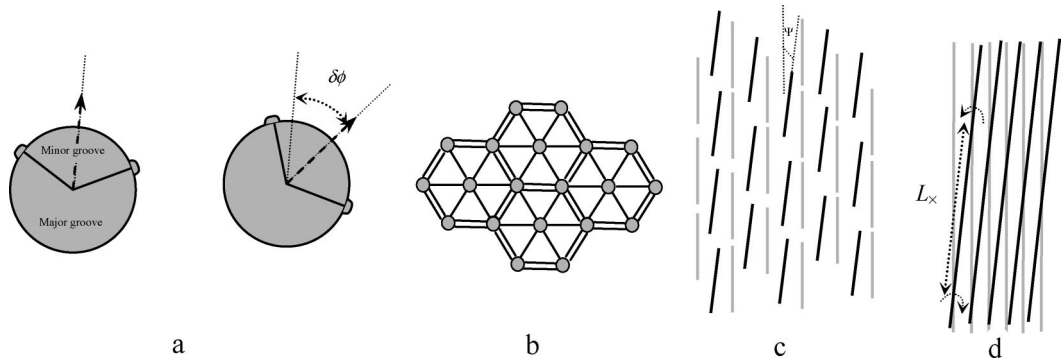

Figure 5. (a) Definition of the mutual azimuthal orientation angle $\delta\phi$ between two DNAs and of orientation of DNA spins. (b) Azimuthal frustrations of DNA molecules on the hexagonal lattice (top view). The difference in azimuthal angles for DNAs connected by two lines is twice as large as for those connected by a single line. (c) Left-handed DNA cholesteric phase of short nucleosomal DNA fragments (black DNA rods are in the top layer). (d) Possible torsional deformations of long DNA molecules in the cholesteric phase.

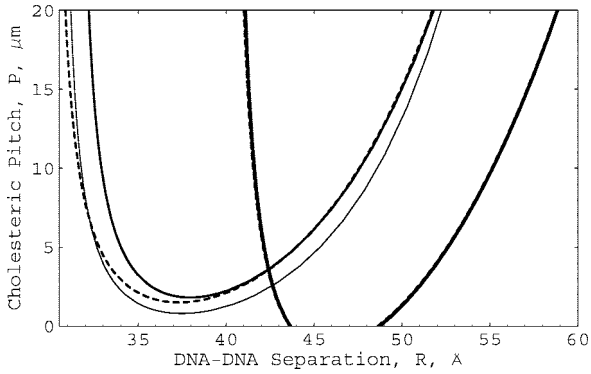

Figure 6. DNA cholesteric pitch as a function of DNA lattice density, as calculated according to eqs 11, 12, and 18) of ref 27. Negative unphysical pitch values are not shown. Parameters: $1/\kappa = 30$, 7, and 3 Å (thin, medium, and thick curves), counterion partitioning between the grooves is minor/major 40%/60%, $a = 9$ Å, $\theta = 0.75$. The Donnan equilibrium for DNA lattice is neglected for dashed and taken into account for solid curves. The curves at $1/\kappa = 3$ Å almost coincide.

3.5. Basic Consequences of the Theory. The theories developed in refs 71, 27, and 13 are the first electrostatic models that relate the microscopic chirality of DNA charges to the formation of DNA CPs. They provide several important consequences.

First, the theory predicts a nonmonotonous dependence of pitch P upon the density of DNA lattice. The absolute pitch values are in qualitative agreement with experiments for realistic DNA parameters, Figure 6. The competition of the first and second helical harmonics of the helix-helix EIs, coming with the opposite signs into the final result for the pitch, is responsible for this nonmonotonous behavior.[13] At larger separations the first harmonic dominates, whereas for denser DNA lattices the second harmonic with a shorter screening length contributes stronger. The sign of the pitch however correspond to right-handed DNA CPs, in clear disagreement with experiments where left-handed DNA CPs are commonly observed.

Second, the DNA CP was suggested to disappear at DNA−DNA separations of $R \lesssim 30$ Å and at $R \gtrsim 40-50$ Å. At large separations, the reason for this are exponentially screened DNA−DNA EIs that provide only weak DNA azimuthal correlations. The latter are smeared out by DNA thermal axial fluctuations and the CP is destroyed.[71,27] At small DNA−DNA distances, the CPs were suggested to turn into columnar hexagonal phases because of pronounced azimuthal frustrations of DNAs on the lattice, Figure 5b. The latter follow from the angular-dependent intermolecular interaction potential.

Namely, the EI energy of two long parallel DNA duplexes can be approximate as the sum of the first helical harmonics[13,79]

$$E(R, \delta\varphi)/L \approx a_0(R) - a_1(R)\cos(\delta\varphi) + a_2(R)\cos(2\delta\varphi) \quad (5)$$

Here $\delta\phi$ is the angle of mutual DNA azimuthal rotation, Figure 5a. The coefficients a_i decay nearly exponentially with R and for higher harmonics the effective decay lengths are shorter, see Figure 1 and eqs A1 and A2 in ref 80. The ground-state of this angular potential at large R corresponds to DNA hexagonal lattice with all molecular spins pointing in the same angular direction. These DNA "spins" are determined by the direction of DNA minor groove. At small R, the DNA lattice is frustrated, Figure 5b, and new degenerate minima of DNA−DNA azimuthal EI energy are realized. Then, the energetic cost of DNA rotations on large angles around the axis is diminished[27] and DNA−DNA azimuthal correlations can be disrupted easier at large [DNA].

4. DNA Cholesteric Pitch and Phase Coexistence

Intuitively, one can expect a left-handed pitch when all counterions adsorbed on DNA are treated as uniformly smeared layer on DNA surface. Such twist direction would make the crossing angle between the phosphate strands on two DNAs larger and thus lower their repulsive EI energy, Figure 2c. On the other hand, if the cations are treated as thin charged strings in DNA grooves, at high amount of added salt and for model helices with large radii, a right-handed pitch can be expected, because strings of cations prefer to be aligned with the strands of DNA phosphates on another molecule, Figure 2d. The theory of ref 27 does predict right-handed twist direction for double-stranded DNA helices.

Note that for the value of parameters used in the model the interactions of parallel DNAs are predominantly repulsive. If they were attractive at separations relevant for DNA CPs, some instabilities would occur in the system. In particular, the assumption about fixed DNA-DNA separations R in the CPs, that are kept constant by the external osmotic stress, can no longer be true. To ensure repulsive interactions, relatively small DNA charge compensation fractions θ and nearly equal partitionings of adsorbed cations between DNA grooves are typically used to plot final results of the model.

4.1. DNA Length Dependence of the Pitch. The pitch of DNA CPs was shown to scale with DNA length as $P \sim L$ in the theory for long DNAs[71] and as

$$P \sim L^2 \quad (6)$$

in a more accurate theory for finite-length DNA fragments.[27] This prediction appears to be inconsistent with a number of

experimental observations, where the pitch of DNA CPs is reported to be nearly independent of DNA length for dense DNA cholesteric assemblies.

One reason for this disagreement can be the fact that the mixtures of relatively long DNAs used in experiments are quite polydisperse. Often, the variation in DNA lengths for some samples exceeds an order of magnitude.[14,81] From these data on polydisperse DNA samples, it is hard to make a definite conclusion about the actual $P(L)$ dependence that could be compared with the theory. Note that no systematic measurements of $P(L)$ variation for monodisperse DNA solutions have been performed.[82,83] It appears however that for very monodisperse mixtures of fd-viruses the pitch dependence observed in experiments[12] does not follow the $P \sim L^2$ law either. On the opposite, the pitch value rather decreases slowly with increase of the virus length, $P \sim L^{-1/4}$.

Another reason could be in assumptions of the model. In the theory, the pitch grows with DNA length because no multiple molecular intersections in neighboring cholesteric layers are allowed by the quadratic energy expansion used, eq 3. The latter works only for small twist angles Ψ, see Figure 5c. Therefore, as DNA length grows and separations between DNA layers are kept constant, there is no other way to ensure the validity of this assumption as to diminish the twist angle.[84] Therefore, the pitch grows rapidly with the DNA length in the model.

As no pronounced $P(L)$ variation is detected in experiments, one can hypothesize that long DNAs, $L \gg l_p \approx 150$ bps, interact effectively as a sequence of quasi-independent segments of the length, Figure 5d

$$L_{\times} \sim R/\sin \Psi \tag{7}$$

Also, it is natural to assume that in CPs made of shorter DNA fragments the azimuthal DNA rotations are easier to perform and the effects of axial thermal fluctuations are more pronounced. However, apparently this has little effect on the pitch values measured, in a wide range of DNA lengths. For realistic values of twist angles between DNA layers in CPs and at relevant DNA densities,[32] $\Psi \approx 0.6°$ and $R \approx 35$ Å, this crossing length is $L_{\times} \sim 1000$ bps, assumed here to be independent of DNA length L.

For DNA fragments that exceed this length, multiple intermolecular crossings occur in cholesteric layers, Figure 5d. Each DNA−DNA crossing will require particular DNA−DNA azimuthal orientations in order to lower the energy of DNA−DNA EIs. Therefore, some torsional deformations of DNA backbone near the contacts with the neighbors are required to keep DNA−DNA azimuthal correlations in the assembly. These deformations correspond to a twisting of some segments of a long DNA and cost DNA twist elastic energy. Therefore, to stabilize the CPs of DNAs with $L \gg 1000$ bps, a higher external osmotic stress should be applied as compared to that for ~150 bp long fragments at the same DNA lattice density. This prediction can be checked in the future experiments.

4.2. Elastic Deformations of DNA Cholesterics. The twist elastic constant of the DNA CPs, Figure 7[27]

$$K_{22} = \frac{\sqrt{3}}{2L} \frac{\partial^2 E_{\Delta}(\Psi)}{\partial \Psi^2} = \frac{\sqrt{3}\langle U_2 \rangle}{2L} \propto L^2 \tag{8}$$

must be positive for the DNA CP to be stable with respect to elastic twist deformations of DNA layers. The Frank elastic twist free energy of the CPs can be written as (per unit volume)[85]

$$F(R) = \frac{K_{22}(R)}{2}\left[\vec{n} \cdot (\nabla \times \vec{n}) + \frac{2\pi}{P(R)}\right]^2 \tag{9}$$

where $\vec{n}$ is the director field. The necessary condition

$$K_{22} > 0 \tag{10}$$

is satisfied for DNA CPs in some region of parameters and for particular DNA lattice densities, Figure 8. In the red regions of Figure 8, the theory predicts $K_{22} < 0$ and DNA twisted phases cannot be stabilized by EIs. Other types interactions not considered here should contribute.

The dependence of K_{22} on the density of DNA lattice typically reveals two different decay exponents, at small and large DNA−DNA separations R, see the curves at $1/\kappa = 7$ Å in Figure 7. The K_{22} can however become negative for intermediate R values, indicating that the DNA CPs stabilized solely by EIs cannot exist there. For large [salt], at $1/\kappa = 3$ Å, the region of $K_{22} < 0$ exists at $R \approx 44-49$ Å corresponding to the region of $P < 0$ in Figure 6. For small [salt], at $1/\kappa = 30$ Å, when the Donnan equilibrium is neglected, the value of K_{22} is only positive in the theory for small R values, while after salt repartitioning is taken into account we get $K_{22} > 0$ for all densities of the DNA lattice.[77]

The actual measurements of K_{22} for DNA CPs via cholesteric-nematic unwinding by the magnetic field are not straightforward because of the negative anisotropy of diamagnetic susceptibility of DNA molecules. The DNAs thus tend to align perpendicular to the magnetic field[32] and not parallel to it, as in the case of PBLG and fd viruses. To our knowledge, no measurements of the twist elastic constant in DNA CPs at different salt contents and external pressures have been performed so far.

The azimuthal rigidity constant k_{ϕ} that describes the energy of DNA rotations by an angle $\delta\phi$ around DNA axis, $k_{\phi}\delta\phi^2/2$, in nearly hexagonal lattice of 6 neighboring DNAs is[27]

$$k_{\phi} = -6\,(u_{01} + 4u_{02}) \tag{11}$$

Constant k_{ϕ} should also be positive by definition and this condition is satisfied outside of magenta regions in Figure 8.

4.3. Donnan Salt Equilibrium in DNA Phase. The salt dependence of P predicted by the theory[27] also does not agree well with experimental data. Namely, it is observed that the region of existence of CPs shifts toward higher DNA densities at higher [salt] in experiments, Figure 3, opposite to what follows from our theory.[86] The correct shift of isotropic−nematic phase transition boundary as a function of [salt] is predicted from the theory of refs 90 and 91, see also ref 92.

Note that the behavior of CPs of other biohelices reveals the same tendencies as [salt] varies. Similar to CPs of DNAs, for fd viruses the region of stability of CPs was shown to shift toward higher densities at higher [salt] n_0. Namely, at $n_0 = 4$

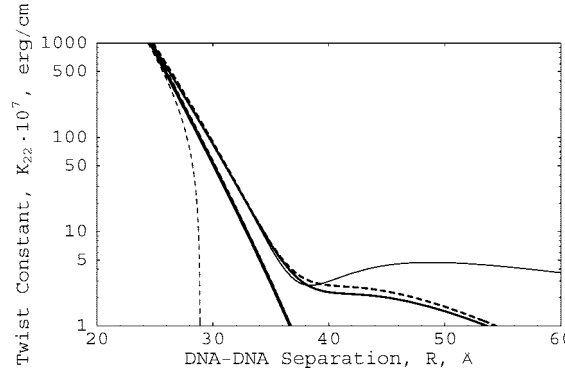

Figure 7. Twist elastic constant of the DNA CPs, as calculated from eq 19 of ref 27. Parameters and notations for the curves are the same as in Figure 6. The representative behavior of K_{22} is at $1/\kappa = 7$ Å. Typical values of twist constant for liquid crystals are $K_{22} \times 10^7 \sim 10$ erg/cm. The curves at $1/\kappa = 3$ Å almost superimpose.

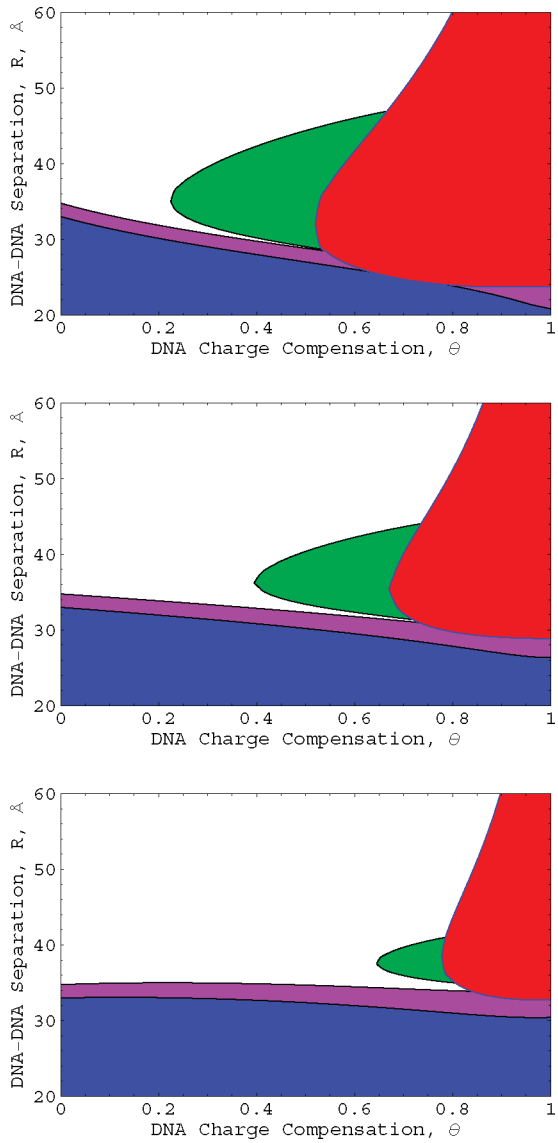

Figure 8. Strong DNA−DNA azimuthal correlations exist in green regions, where the energy of azimuthal rotation for a 146 bp DNA fragment on DNA hexagonall lattice is larger than k_BT. The DNA CPs cannot be stabilized by EIs in the red regions, where the elastic constant $K_{22} < 0$. Part of the green domains are overlapped by the red ones. The cholesteric pitch P is negative (left-handed phases) inside blue and red regions. The effective rigidity constant is negative, $k_\phi < 0$, in the magenta domains, which include blue domains completely and go down to small R. Cation partitionings between DNA grooves minor/major are 10/90, 30/70, and 40/60, for graphs from top to bottom; $a =$ 9 Å, $1/\kappa = 7$ Å. The results of ref 27 are used, with the Donnan equilibrium taken into account.

mM the CP exists at $15 \lesssim C \lesssim 50$ mg/mL, whereas at 68 mM of salt the CP is stable at $20 \lesssim C \lesssim 150$ mg/mL. At higher C, smectic phases are detected, and this transition is accompanied by a slight increase of P. Also, similarly to DNA, the cholesteric pitch value for assemblies of fd viruses is typically considerably smaller at larger salt amounts, see Figure 3 in ref 6. The twist elastic constant was shown to vary with virus concentration in the range $0.2 \lesssim K_{22} \times 10^7 \lesssim 1.4$ erg/cm.

The original theory of ref 27 however does not account for the effects of salt equilibrium in dense DNA CPs. When the Donnan salt equilibrium is taken into account,[97−99] the effective screening length in spaces between DNAs becomes a function of [DNA]. The [counterion] is regulated by the average electrostatic potential in the aqueous phase between DNAs. This potential is maintained at the value that preserves the neutrality of DNA aggregate together with all ions. Cations accumulate in solution between DNAs in dense DNA phases, diminishing the effects of n_0 variation. Ion concentrations can reach ∼0.5−1 M in spaces between DNAs for very dense lattices. The reciprocal screening length in solution between DNAs on the hexagonal lattice is[80,100]

$$\kappa_D(R) = \kappa\left[1 + \frac{16 l_B^2 (1-\theta)^2}{\kappa^4 b^2 \left(R^2 \frac{\sqrt{3}}{2\pi} - a^2\right)^2}\right]^{1/4} \qquad (12)$$

Here $\kappa = (8\pi l_B n_0)^{1/2}$ is the inverse Debye length in bulk solution, $l_B \approx 7.1$ Å is the Bjerrum length in water, $b \approx 1.7$ Å is the average charge−charge separation on double stranded B-DNA, and $a \approx 9$ Å is the DNA radius.

At low n_0, the theory of DNA CPs without Donnan equilibrium results in unphysical pitch values and in unstable CPs for all densities of DNA lattice (the curve is not shown in Figure 6). When we take salt equilibrium into account, stable DNA CPs follow from the theory at low salinities, thin solid curve in Figure 6. As [salt] in the bulk grows, the effects of redistribution of ions in the DNA phase are progressively diminished. At $n_0 = 1$ M, for instance, the cholesteric pitch is almost indistinguishable for situations with and without Donnan equilibrium.

Note that these stronger screening effects due to salt equilibrium can be partially compensated by lowering the dielectric constant in concentrated electrolytes. Namely, for NaCl solutions the dielectric constant decreases with n_0 as[101] $\varepsilon(n_0) \approx 80 - 11[n_0]$, where n_0 is [salt] in M. We take this dielectric saturation effect into account in Figures 6 and 8.

The nonmonotonous behavior of $P(R)$ and pitch absolute pitch values obtained from the theory[27] are in qualitative agreement with experimental data for realistic parameters of DNA charge pattern. For repulsive DNA−DNA interactions, the pitch is typically right-handed, Figure 6, being opposite to the direction of twisting as interpreted from the circular dichroism data. The theory can result also in left-handed pitch, the blue regions in Figure 8, that extend for R down to DNA−DNA contact. The $P < 0$ regions are realized at small DNA−DNA separations R (where $u_{11} + u_{12} > 0$ and $u_{20} + u_{21} + u_{22} > 0$); these regions are inside the magenta domains with $k_\phi < 0$. The pitch can also be negative at intermediate R values that are realized for $u_{11} + u_{12} < 0$ and $u_{20} + u_{21} + u_{22} < 0$. These regions are inside the red domains in Figure 8. As both domains of negative pitch correspond to unphysical situations, left-handedly twisted DNA phases observed in experiments do not follow from this theory.

4.4. DNA Azimuthal Correlations. As noted in Introduction, relatively strong azimuthal correlation are necessary for existence of DNA CPs. We have estimated the strength of DNA-DNA azimuthal correlations for DNA hexagonal lattices at different densities. To quantify the strength of correlations in CPs of standard DNA nucleosomal fragments, we use as a criterion the DNA-DNA separations R at which the energy to rotate azimuthally a 146 bp long DNA as a whole around its axis on the lattice is equal to k_BT. We have used here the expression for DNA-DNA interaction energy,[27] modified due to salt equilibrium between bulk reservoir and DNA phase.

We obtain that well neutralized DNAs with a large fraction of cations in DNA major groove possess strong correlations in experimentally relevant region of R, the green regions in Figure 8. Part of these green domains is overlapped by the red domains with $K_{22} < 0$. Outside of the green domains, the correlations are weak and thermal fluctuations are capable

to wash out the effects of chiral DNA−DNA EIs. The green domains at physiological salt conditions are located at $R \sim 30-45$ Å, i.e., at the same DNA lattice densities where DNA CPs are detected in experiments. Such DNA CPs imply strong azimuthal correlations. The regions of strong correlations are bounded at large R because EIs are screened. Weakening of correlations at small R is caused by interaction-induced azimuthal DNA frustrations on the lattice that could trigger cholesteric-to-hexagonal phase transition at large [DNA].

As [salt] in the bulk increases, the region of strong correlation shrinks and eventually disappears: at $n_0 = 1$ M for instance the DNA−DNA EIs are very weak and k_ϕ is considerably smaller that 0.01 k_BT for all DNA−DNA distances. The assumption of strong correlations for P derivation is violated in this regime and the curves in Figures 6 and 7 at $1/\kappa \approx 3$ Å are shown only for illustrative purposes.

5. Discussion and Open Questions

The extended introduction of the paper is supposed to underline the complexity of the phenomenon of formation of dense liquid crystalline twisted DNA phases. We overview a number of experimental data on DNA CPs, in particular, on DNA cholesteric pitch dependence on salt conditions and external pressure. We show that the mutual alignment of DNA molecules is affected by many factors, including salt composition, DNA length, DNA charge pattern, DNA-bound charged polymers, temperature, DNA supercoiling, etc. All these parameters are almost impossible to account for within a single theoretical model.

The motivation for the theoretical part of this study is to show the advantages and drawbacks of modern theories of chiral EIs of biohelices, in application to CPs of DNAs. Despite the fact that the sense of cholesteric pitch obtained from the theory is opposite to that is commonly reported in experiments, the absolute pitch values and its dependence on DNA lattice density are in qualitative agreement with the experimental data. This discrepancy might come from the effects of other types of interactions, neglected in the present study. A combined theory of electrostatic and steric DNA−DNA forces is the next step toward a better understanding of DNA CPs.

Still, we use the theory of DNA−DNA EIs[71,27] as the only model available in the literature that couples the molecular details of DNA structure and its charge pattern to the macroscopic parameters of DNA cholesterics. We have calculated the dependence of DNA cholesteric pitch on [salt] and DNA lattice density, with the Donnan salt equilibrium taken into account. Using the same theory, we have rationalized the strength of DNA−DNA azimuthal correlations in DNA CPs, defined the regions of existence of DNA twisted CPs stabilized by EIs, and discussed the possible senses of DNA cholesteric twist.

As a final comment on EIs in CPs of different biohelices, we note here that the densities of CPs of DNA and of helical viruses appear to be very different. In DNA CPs, the molecular surfaces are separated typically by a couple of Debye lengths. For M13 fd-like viruses at ∼50 mg/mL dilution, however, the virus surface-to-surface distances are ∼200 Å that is much longer than the Debye length of $1/\kappa \sim 10-20$ Å used in experiments.[22] The virus−virus EIs should be fully screened in this regime. One can argue that at these low [virus] the fluctuations of viral axis are capable to bring dynamically two viruses into much closer contacts that those prescribed by average virus density.[102] It was indeed shown within a statistical theory that, when averaged over all virus orientations in space, the EIs do result in formation of CPs with pitch values of $50-100$ μm.[22] It is however unlikely that such temporal contacts of viruses can ensure their substantial azimuthal correlations in dilute viral suspensions at relatively high salinities.

Acknowledgment. I thank E. Grelet, D. J. Lee, A. Leforestier, F. Livolant, S. V. Malinin, A. Minsky, and J. Widom for discussions and anonymous referee for helpful comments. I acknowledge the support by the Deutsche Forschungsgemeinschaft (DFG), Grant CH 707/2-1.

References and Notes

(1) Livolant, F.; Leforestier, A. *Prog. Pol Sci.* **1996**, *21*, 1115.
(2) Leforestier, A. *Comptes Rendus Chim.* **2008**, *11*, 229.
(3) Livolant, F.; Maestre, M. F. *Biochemistry* **1988**, *27*, 3056.
(4) Salyanov, V. I.; et al. *Mol. Bio.* **1995**, *28*, 196.
(5) Yu, M.; et al. *Liq. Cryst.* **1988**, *3*, 1443.
(6) Dogic, Z.; Fraden, S. *Macromolecules* **2000**, *16*, 7820.
(7) Barry, E.; et al. *Phys. Rev. Lett.* **2006**, *96*, 018305.
(8) Robinson, C. *Tetrahedron* **1961**, *13*, 219.
(9) Dupre, D. B.; Duke, R. W. *J. Chem. Phys.* **1975**, *63*, 143.
(10) Bouligand, Y.; Livolant, F. *J. Phys. (Paris)* **1984**, *45*, 1899.
(11) Fraden, S.; et al. *Phys. Rev. Lett.* **1989**, *63*, 2068.
(12) Grelet, E.; Fraden, S. *Phys. Rev. Lett.* **2003**, *90*, 198302.
(13) Kornyshev, A. A.; Lee, D. J.; Leikin, S.; Wynveen, A. *Rev. Mod. Phys.* **2007**, *79*, 943.
(14) Livolant, F. *Eur. J. Cell. Biol.* **1984**, *33*, 300.
(15) Leforestier, A.; Livolant, F. *Biophys. J.* **1993**, *65*, 56.
(16) In dinoflagellates, for instance, the chromosome has a cylindrical shape ($0.3-0.7$ μm in width and $1-2$ μm in length) and consists of a single DNA, Figure 1d. The cholesteric axis is parallel to the chromosome axis and the left-handed DNA pitch is $P \sim 200-400$ nm,[14] much smaller than that measured in vitro.
(17) Straley, J. P. *Phys. Rev. A* **1976**, *14*, 1835.
(18) Green, M. M.; et al. *Science* **1995**, *268*, 1860.
(19) Branden, C.; Tooze, J. *Introduction to protein structure*; Garland Publishers: New York, 1991.
(20) Harris, A. B.; Kamien, R. D.; Lubensky, T. C. *Rev. Mod. Phys.* **1999**, *71*, 1745.
(21) Pelta, J.; Durand, D.; Doucet, J.; Livolant, F. *Biophys. J.* **1996**, *71*, 48.
(22) Tombolato, F.; Ferrarini, A.; Grelet, E. *Phys. Rev. Lett.* **2006**, *96*, 258392.
(23) Rau, D. C.; Parsegian, V. A. *Biophys. J.* **1992**, *61*, 260.
(24) Cherstvy, A. G.; Kornyshev, A. A.; Leikin, S. *J. Phys. Chem. B* **2002**, *106*, 13362.
(25) Brenner, S. L.; Parsegian, V. A. *Biophys. J.* **1974**, *14*, 327.
(26) Cherstvy, A. G.; Kolomeisky, A. B.; Kornyshev, A. A. *J. Phys. Chem. B* **2008**, *112*, 4741.
(27) Kornyshev, A. A.; Leikin, S.; Malinin, S. V. *Eur. Phys. J. E* **2002**, *7*, 83.
(28) Kassapidou, K.; et al. *Macromol.* **1985**, *28*, 3230.
(29) Rill, R. L.; Strzelecka, T. E.; Davidson, M. W.; van Winkle, D. H. *Physica A* **1991**, *176*, 87.
(30) Lennard, M.; et al. *Polymer* **2001**, *42*, 5823.
(31) van Winkle, D. H.; et al. *Macromol.* **1990**, *23*, 4140.
(32) Stanley, C. B.; Hong, H.; Strey, H. H. *Biophys. J.* **2005**, *89*, 2552.
(33) Intuitively, at higher T one expects stronger thermal fluctuations, weaker chiral interactions, and thus larger P values. On the other hand, the dielectric constant of water decreases almost linearly with T between 0 and 100°, $\varepsilon \approx 80-0.4(T-293)$,[34] that can give rise to stronger EIs at higher T. This decrease of ε with T alone *cannot* account for a dramatic decrease of P with T observed in DNA solutions of multivalent cations and some stronger effects should contribute. One can hypothesize, for instance, that some changes in spermidine binding onto DNA upon increase of T could induce this lowering of P.
(34) Knowlton, A. E., Ed.; *Standard Handbook for Electrical Engineers*, 8th ed.; McGraw-Hill Book Company: New York, 1949; sec. 4−583.
(35) Yu. M.; Yevdokimov, *Mol. Biol.* **2002**, *36*, 419.
(36) Samori, B.; et al. *Int. J. Biol. Macromol.* **1993**, *15*, 353.
(37) Minsky, A. *Chirality* **1998**, *10*, 405.
(38) Minsky, A. personal communication.
(39) Calle, A.; et al. *J. Biomol. Str. Dyn.* **2002**, *20*, 99.
(40) Cesare-Marincola, F.; Saba, G.; Lai, A. *Phys. Chem. Chem. Phys.* **2003**, *5*, 1678.
(41) Salyanov, V. I.; et al. *Mol. Biol.* **2002**, *36*, 699.
(42) Reich, Z.; Wachtel, E. J.; Minsky, A. *Science* **1994**, *264*, 1460.
(43) For long linear plasmid DNA the pitch is right-handed at 0.8 M of salt, left-handed at 2.2 M, an again right-handed in the presence of 10 mM of $MgCl_2$ in solution, Figure 4 of ref 37. The same DNAs forming

right-handed supercoiled plasmids form left-handed CPs. Also, the pitch sign does not change with T for linear DNAs, while CP of supercoiled DNAs reveal pitch inversion at about 60° C. The change in supercoiling sense with T is likely to be the reason for this pitch reversal.[37]

(44) Reich, Z. *Biochemistry* **1994**, 33.
(45) Ohyama, T. *BioEssays* **2001**, *23*, 708.
(46) Pennings, S.; et al. *J. Mol. Biol.* **1989**, *207*, 183.
(47) Costanzo, G.; et al. *J. Mol. Biol.* **1990**, *216*, 363.
(48) Travers, A.; Klug, A. *Nature* **1987**, *327*, 280.
(49) Zhurkin, V. B. *FEBS Lett.* **1983**, *158*, 293.
(50) Drew, H. C.; Travers, A. A. *J. Mol. Biol.* **1985**, *186*, 773.
(51) Segal, E. *Nature* **2006**, *442*, 772.
(52) Shrader, T. E.; Crothers, D. M. *Proc. Natl. Acad. Sci.* **1989**, *86*, 7418.
(53) Calladine, C. R.; et al. *J. Mol. Biol.* **1988**, *201*, 127.
(54) Olson, W.; Gorin, A.; Lu, X.; Hock, L.; Zhurkin, V. *Proc. Natl. Acad. Sci. U.S.A.* **1998**, *95*, 11163.
(55) Gorin, A. A.; Zhurkin, V. B.; Olson, W. K. *J. Mol. Biol.* **1995**, *247*, 34.
(56) Becker, N. B.; Wolff, L.; Everaers, R. *Nucleic Acids Res.* **2006**, *34*, 5638.
(57) Widom, J. private communication.
(58) Klimenko, S. M.; et al. *J. Mol. Biol.* **1967**, *23*, 523.
(59) Earnshaw, W. C.; Harrison, S. C. *Nature* **1977**, *268*, 598.
(60) Lepault, J.; et al. *EMBO J.* **1987**, *6*, 1507.
(61) Cerritelli, M. E.; et al. *Cell* **1997**, *91*, 271.
(62) Blanc, N. S.; et al. *J. Struct. Biol.* **2001**, *134*, 76.
(63) Cherstvy, A. G. *J. Phys.: Condens. Matter* **2005**, *17*, 1363.
(64) Kornyshev, A. A.; Leikin, S. *J. Chem. Phys.* **1997**, *107*, 3656.
(65) Cherstvy, A. G. *J. Phys. Chem. B* **2007**, *111*, 7914.
(66) Tombolato, F.; Ferrarini, A. *J. Chem. Phys.* **2005**, *122*, 054908.
(67) Manning, G. S. *J. Phys. Chem. B* **2007**, *111*, 8554, and references cited therein.
(68) Cherstvy, A. G.; Kornyshev, A. A.; Leikin, S. *J. Phys. Chem. B* **2004**, *108*, 6508.
(69) Cherstvy, A. G.; Everaers, R. *J. Phys.: Condens. Matter* **2006**, *18*, 11429.
(70) Kornyshev, A. A.; Leikin, S. *Phys. Rev. Lett.* **2000**, *84*, 2537.
(71) Kornyshev, A. A.; Leikin, S. *Phys. Rev. E* **2000**, *62*, 2576.
(72) Onsager, L. *Ann. N.Y. Acad. Sci.* **1949**, *51*, 627.
(73) Lee, D. J. work in preparation.
(74) Wynveen, A.; Lee, D. J.; Kornyshev, A. A. *Eur. Phys. J. E.* **2005**, *16*, 303.

(75) A simple estimate for the strength of chiral EIs of randomly sequenced DNA fragments can be as follows. In the theory of ref 27, both the strands of DNA phosphates and counterions adsorbed in DNA grooves are considered as infinitely thin charged helical lines. Sequence specificity of DNA twist angles[54] results in nonideally helical DNA structures that have to be modeled differently. Neglecting the fact of possible DNA interaction-induced torsional adjustment, the skewed helices with such nonideal patterns can be approximated by smeared charge distributions. Namely, both the strands of phosphates and of adsorbed cations can be considered as helical stripes of a finite thickness w, instead of being thin helices. This Debye-Waller charge smearing diminishes the structure factor $^{p}(mg)$, that is the Fourier component of the helical charge distribution on DNA,[27] as follows $p(mg) \rightarrow p(mg)e^{-m^2g^2w^2/4}$, where $g = 2\pi/H$. The values of K_t, k_ϕ, and K_{22}, that are proportional to $p(mg)^2$, decrease correspondingly. The cholesteric pitch value remains however unaffected because according to eq 4 $p(mg)$ disappears from the final result for the pitch. Thus, no predictions for the pitch of CPs of homologous *vs.* randomly sequenced DNAs can be drawn from such simple charge smearing.

(76) Baldwin, G. S.; et al. *J. Phys. Chem B* **2008**, *112*, 1060.

(77) A clear non-monotonous behavior of P on the density of assembly is not inherent for other helices. For instance, for CPs of PBLG the cholesteric pitch decreases dramatically with polymer concentration C in a wide range, following the relation $P \propto C^{-(1.8 \div 2)}$.[9] The value of twist elastic constant, K_{22}, that was monitored via unwinding of cholesterics into nematics by the applied magnetic field, increases however only slightly with C. The pitch was shown to increase also with temperature, while K_{22} values decrease considerably with T. The pitch decreases also with polymer length, L. The value of K_{22} grows almost 100 times, from $K_{22} \times 10^7 = 0.6$ to $K_{22} \times 10^7 = 58$ erg/cm, as L increases just by a factor of two.[9] In different solvents, the pitch value is $30 \lesssim P \lesssim 80$ μm, while the K_{22} can vary as $0.6 \lesssim K_{22} \times 10^7 \lesssim 5.4$ erg/cm. Depending on the solvent, even the inversion of the twist sense is observed. Similar to PBLG, for CPs of fd viruses,[6] the cholesteric pitch varies in a wide range of [virus] C as $P \propto C^{-(1.65 \div 1.1)}$, with the absolute value of the exponent growing with [salt] n_0. Theoretically, the twist elastic constant for the nematic phase of hard rods was shown to scale as $K_{22} \propto L^2C$ in the theory of ref 78 and as $K_{22} \propto L^4C^2$ in the model of ref 17. So, a very weak dependence of $K_{22}(C)$, a strong variation of the cholesteric pitch with polymer density, and a strong dependence of parameters of CPs on solvents, observed for PBLG CPs in experiments,[9] do not agree with the predictions of existing theories for ordering of hard noninteracting rods in concentrated solutions. The $K_{22}(C)$ and $P(C)$ variations observed can in some cases be qualitatively described in the theory of ordered semi-flexible chains [78].

(78) Odijk, T. *J. Phys. Chem.* **1987**, *91*, 6060.
(79) Harreis, H. M.; et al. *Phys. Rev. Lett.* **2002**, *89*, 018303.
(80) Cherstvy, A. G.; Kornyshev, A. A. *J. Phys. Chem. B* **2005**, *109*, 13024.
(81) Livolant, F. *J. Phys. (Paris)* **1986**, *47*, 1605.
(82) Leforestier, A. private communication.
(83) Goldar, A.; Thomson, H.; Seddon, J. M. *J. Phys. Cond. Matt.* **2008**, *20*, 035102.
(84) Lee, D. J. private communication.
(85) Stephen, M. J.; Straley, J. P. *Rev. Mod. Phys.* **1974**, *46*, 617.

(86) The shift of the density of stable DNA CPs towards higher DNA concentrations at higher salinities of solution is akin of the change in density observed for spontaneously formed hexagonal assemblies of TMV viruses.[87,88] Experimentally, the equilibrium virus–virus separations were shown to decrease at higher salt concentrations. Theoretically, the equilibrium lattice density of TMV assembly was suggested to originate from a competition of repulsive electrostatic interactions between the viral coat proteins and attractive short-range van der Waals forces. Then, as [salt] increases, the repulsive coulombic forces are screened better and virus-virus short-range salt-independent attraction results in a closer contact of viruses[89].

(87) Parsegian, V. A.; Brenner, S. L. *Nature* **1976**, *259*, 632.
(88) Millman, B. M.; et al. *Biophys. J.* **1984**, *45*, 551.
(89) Brenner, S. L.; McQuarrie, D. A. *Biophys. J.* **1973**, *13*, 301.
(90) Stroobants, A.; Lekkerkerker, H. N. M.; Odijk, Th. *Macromolecules* **1986**, *19*, 2232.
(91) Odijk, Th. *Macromolecules* **1986**, *19*, 2313.

(92) The influence of EIs of uniformly charged long rods on position of isotropic-nematic phase boundaries was studied in ref 90. In this paper, the rod−rod EIs eq 2 were incorporated in the Onsager theory of nematic ordering.[72] The concepts of effective rod diameter D_{eff} and of electrostatic twisting force have been utilized. For low [salt], lower concentrations of rods are required to provoke the nematic alignment as compared to the uncharged rods. The $C_{i,a}$ decrease with DNA length, almost like $1/L$ for 150−500 bp long DNAs,[93] reaching a plateau for longer fragments. Typically, the $C_{i,a}$ calculated from the theory for long rods are lower than observed for ∼150 bp DNA fragments.[29] It was also suggested that the DNA released from nucleosomes are naturally curved that might result in increase of $C_{i,a}$ due to steric constraints. Weakly attractive interactions between DNAs were also suggested to lower $C_{i,a}$, favoring DNA−DNA zipper effects. For nematic assemblies of fd-viruses, the concept of effective diameter and chain flexibility were applied to describe the [salt]-dependence of $C_{i,a}$.[95] Such theory becomes however less satisfactory at low salt, when the ratio L/D_{eff} decreases.[96]

(93) Rill, R. L. *J. Biol. Chem.* **1983**, *256*, 250.
(94) Merchant, K.; Rill, R. L. *Biophys. J.* **1997**, *73*, 3154.
(95) Purdy, K. R.; Fraden, S. *Phys. Rev. E.* **2004**, *70*, 061703.
(96) Purdy, K. R.; et al. *Phys. Rev. E.* **2003**, *67*, 031708.
(97) Donnan, F. G. *Chem. Rev.* **1924**, *1*, 73.
(98) Denton, A. R. *Phys. Rev. E* **2007**, *76*, 051401.
(99) Deserno, M.; von Gruenberg, H. H. *Phys. Rev. E* **2002**, *66*, 011401.
(100) Poghossian, A.; et al. *Sens. Actuators B* **2005**, *111−112*, 470.
(101) Hasted, J. B.; Ritson, D. M.; Collie, C. H. *J. Chem. Phys.* **1948**, *16*, 1.
(102) Grelet, E. personal communication.

JP801220P